View metadata, citation and similar papers at core.ac.uk
brought to you by CORE
provided by CiteSeerX

Proceedings of IMECE2002
ASME International Mechanical Engineering Congress & Exposition
November 17–22, 2002, New Orleans, Louisiana

IMECE2002-39000

A New Self-Adjusting CVT Configuration Using Compliant Mechanisms

Myles T. Christensen
Associate Design Engineer
Graco Children's Products
Elverson, PA
mtchristensen@gracocorp.com

Spencer P. Magleby, Larry L. Howell, Robert H. Todd
Mechanical Engineering
Brigham Young University
Provo, UT
magleby@byu.edu, lhowell@et.byu.edu, todd@byu.edu

Clint Mortensen
BMD & Advanced Programs
Raytheon Missile Systems
Tuscon, AZ
cmortensen@west.raytheon.com

ABSTRACT

This paper introduces a new configuration of a Continuously Variable Transmission (CVT) that is self-adjusting and designed as a compliant mechanism. This new configuration is called the Pivot-Arm CVT. The criteria for classification as a Pivot-Arm CVT is discussed. An analytical model describing the performance of the Pivot-Arm CVT is developed. Special design considerations which may be useful in implementing Pivot-Arm CVTs are introduced and explained. The Pivot-Arm CVT model is validated through controlled testing of two Pivot-Arm CVT prototypes.

Introduction

In the area of power transmission, there are several advantages that make the Continuously Variable Transmission (CVT) appealing to designers. The main advantage of the CVT, compared to a traditional transmission with fixed gearing, is the ability to run the input source at the precise speed that corresponds to maximum power. Current CVTs exist in all sorts of vehicles, from typical internal combustion engine cars and trucks to hybrid and purely electric vehicles. There are CVTs in snowmobiles, ATVs and lawn mowers. CVTs are also used in industrial machine tool drives (Beachley and Frank, 1979).

Development efforts at Brigham Young University have led to a configuration for a CVT that is extremely simple and lightweight, yet does not rely on friction as the torque-carrying medium. Designs for this CVT have progressed from simple compliant arms to a parallel motion configuration (Mortensen, 2000) and finally a generalized design for a "Pivot -Arm" configuration. This Pivot-Arm CVT was designed specifically for the eventual application to a bicycle drive train. The potential advantages of the Pivot-Arm CVT are the attributes needed in a bicycle drive train: lightweight design and efficient power transmission.

A characteristic of the Pivot-Arm CVT that is critical to its application to a bicycle drivetrain is that it was designed to be self-adjusting. This means that the CVT's transmission ratio changes based on input torque. The advantage of this type of control mechanism over typical methods of controlling the transmission ratio is that it does not involve any electronic monitoring system, nor does it require any user intervention. The feedback and control mechanism is part of the CVT's design itself, and it is completely mechanical.

The purpose of this paper is to introduce the pivot-arm CVT including possible configurations and design constraints, and present a performance model for this new configuration. Once the performance model for the Pivot-Arm CVT is developed, it will be validated by testing the performance of prototype CVTs.

The Pivot-Arm CVT is a new type of CVT that has some unique characteristics compared to current CVTs. The description and model contained in this paper will help designers to implement this type of transmission. The paper first presents a brief background on selected CVTs to serve as a comparison to the Pivot-Arm configuration. Following the comparisons a definition for the pivot arm configuration is given.

Background

In this section a review of general CVT classifications is given followed by a discussion of self-adjusting CVTs. Finally, because compliant mechanisms are central to this CVT research,

Copyright © 2002 by ASME

Downloaded From: https://proceedings.asmedigitalcollection.asme.org on 06/28/2019 Terms of Use: http://www.asme.org/about-asme/terms-of-use

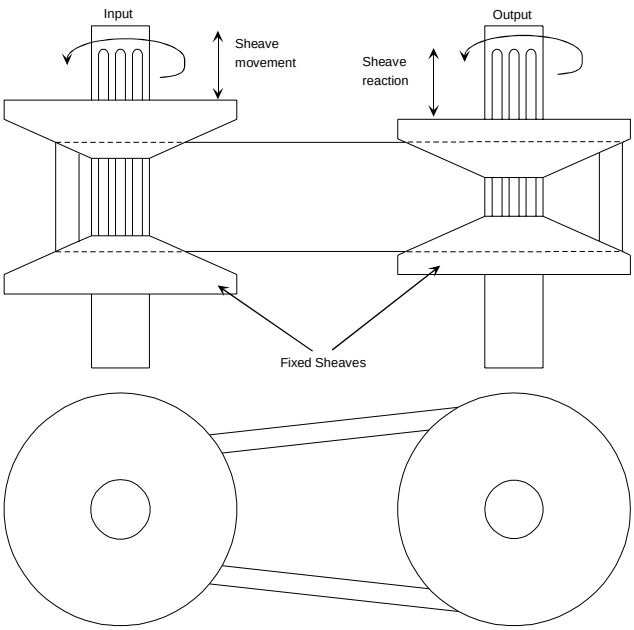

Figure 1: Variable-pitch sheave CVT configuration

there is a discussion of compliant mechanism theory and the Pseudo-Rigid Body Model for compliant mechanism analysis.

Singh and Nair (1992) define a continuously variable transmission as a transmission whose speed ratio can be changed continuously. In other words, a CVT can operate at any speed ratio within its design parameters. In characterizing the operational limits of a CVT, the ratio range is often used. This parameter is the ratio of the maximum to minimum output speeds for a fixed input speed (Beachley and Frank, 1979). In keeping with standard notation, this ratio will be referred to as R.

There are several classifications of CVTs that are relevant to the current work. Friction, and traction types will be reviewed to serveas a comparison to the Pivot Arm configuration.

Friction CVTs are characterized by the use of friction to transfer power. There are several types of friction CVTs. Among those are rubber V-belts, metallic V-belts, and flat rubber belts. The V-belt types all use a pair of variable pitched sheaves in which the belts ride. The effective pitch of the sheave is varied by changing the distance between the two halves of the sheave. As the halves of the sheave move toward each other, the belt is pushed up to a larger diameter. The opposite happens as the halves are spread apart. This control of the effective diameter at which the power is transferred to and from the belt is what gives the transmission its continuously variable characteristic. Figure 1 shows a diagram of a pair of variable pitch sheaves. Rubber V-belt CVTs are commonly used in snowmobile transmissions and machine tools.

The metallic V-belt is actually made up of metal blocks held together by several steel bands (See Figure 2). This type of belt

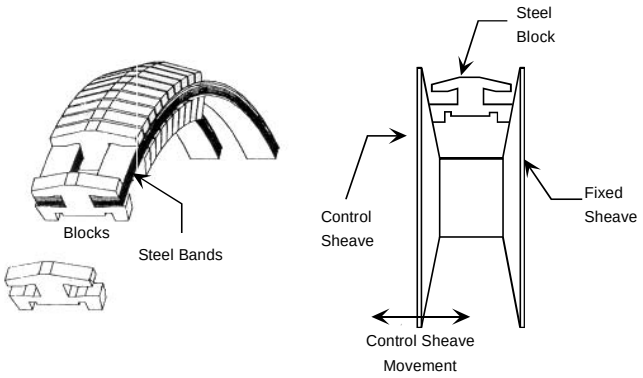

Figure 2: Steel push belt and sheave (from Kluger and Fussner, 1997)

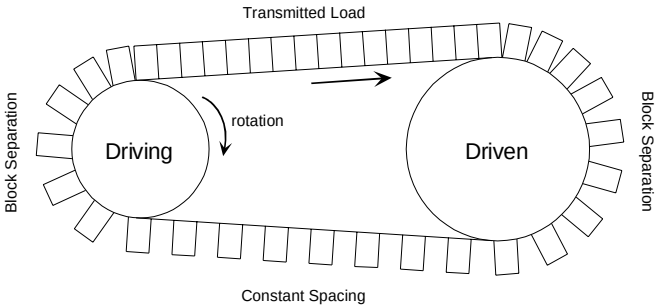

Figure 3: Block loading and spacing in steel push belt

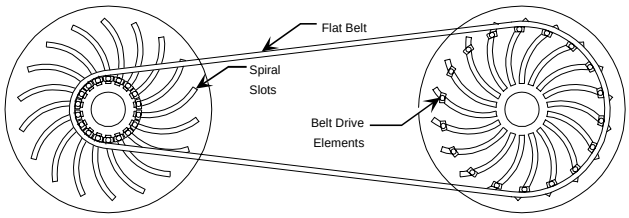

Figure 4: Flat rubber belt CVT configuration

is more suited to a compression load, so the belt is loaded in the way shown in Figure 3. The steel V-belt (or the push type belt) CVT has efficiencies between 94% and 97% depending on the torque level, with the efficiency increasing as torque increases (Kluger and Fussner, 1997).

The flat belt CVT has a much different configuration than the V-belt types. Figure 4 shows a diagram of a flat belt CVT system. The belt rides on a series of belt drive elements which are held at a certain diameter by a pair of plates with opposing spiral slots. As the plates rotate with respect to each other, the belt drive elements are forced to a larger or smaller diameter depending on the direction of rotation. Two of these pairs of plates are used together to form the CVT as shown in Figure 4. Kluger and Fussner, 1997, state that this type of CVT has efficiencies over 97% at high output speeds and power levels.

Copyright © 2002 by ASME

Downloaded From: https://proceedings.asmedigitalcollection.asme.org on 06/28/2019 Terms of Use: http://www.asme.org/about-asme/terms-of-use

For lower speeds and lighter loads, belt efficiencies drop to around 94%.

Traction drives have often been classified with friction drives because they appear to use the friction between two bodies to transmit power. However, the traction drive actually relies on a phenomena called elastohydrodynamic fluid film contact to transmit the power. The traction drive is made up of a set of hardened metal rolling bodies with a fluid film between them. As the drive operates, the film is subjected to extreme compression. The instantaneous viscosity, and thus shear strength, of the fluid increases dramatically due to this compressive stress. It is the shear strength of the fluid that allows power to be transferred. A common configuration is the use of an idler. As the idler changes its orientation, the effective engagement radius on the input and output shafts change, thus giving the transmission its continuous nature. Traction drives are typically used in low-power yard equipment, machine tools, and some automobiles.

As will be shown later, the Pivot-Arm CVT does not fit into any of the usual classifications of CVTs. Because of the uniqueness of this design, we have made a new classification that will be presented as part of the section on model development.

Self-Adjusting CVTs

There are many CVTs which use feedback and control mechanisms to change the CVT's transmission ratio. They fall into two main categories: those that sense the speed of the system, and those that sense the torque of the system (Oliver et al., 1973). The terms "torque sensing" or "speed controlled" are often used to describe these types of CVTs. For the purpose of this paper, both of these types will be referred to as "self-adjusting" CVTs. The category of self-adjusting CVTs is introduced here because of its relevance to the pivot-arm CVT design. CVTs that use electronics as a feedback and control mechanism will not be examined.

Oliver et al., (1973) examine a CVT system which uses both a speed sensing and a torque sensing configuration. The speed sensing apparatus is mounted to the driver sheave, and the torque sensing system is part of the driven sheave. The driver sheave set-up is shown in Figure 5. The CVT senses the speed by the use of the centrifugal garter spring. As the speed in the drive axle increases, the garter spring is forced outward which forces the sheave halves closer together. Oliver et al. develop an expression for the speed of the driver sheave in terms of the effective diameter of the belt in the pulley. This expression shows that there is a direct correlation between the input speed (speed of the driver pulley) and the transmission ratio (effective diameter on the driver pulley). This relationship is what makes this sheave mechanism self-adjusting.

Figure 6 shows the driven sheave assembly from the work of Oliver. This is a torque sensing CVT. As the output torque

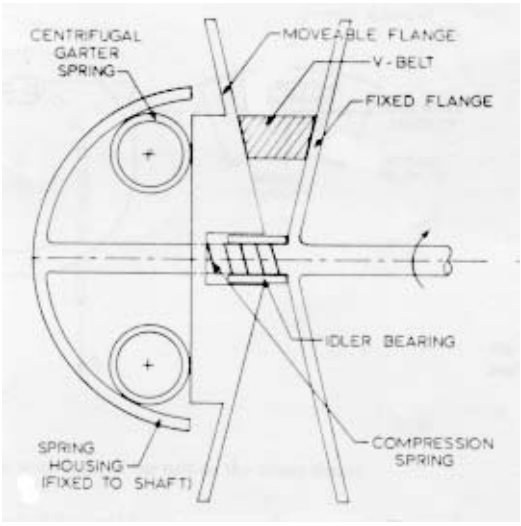

Figure 5: Speed sensing adjustable sheave (from Oliver et al., 1973)

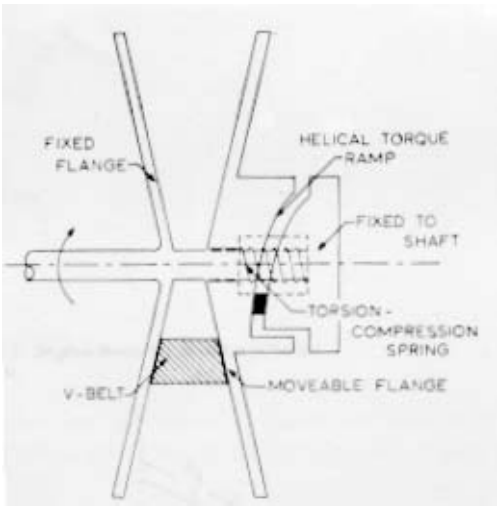

Figure 6: Torque sensing adjustable sheave (from Oliver et al., 1973)

requirements increase, the moveable flange rotates slightly with respect to the shaft. This slight rotation causes the moveable flange to ride up the helical torque ramp causing the sheave halves to be forced together. Oliver, also developed and validated a set of equations predicting the performance of this CVT (Oliver et al., 1973). This set of equations includes an expression for the axial force on the sheave in terms of the tension difference in the belt and the effective diameter of the belt in the sheave. The term for the tension difference is a component of the torque, and the effective diameter determines the transmission ratio. This relationship between torque and transmission ratio is the key to predicting the performance of this self-adjusting CVT.

Copyright © 2002 by ASME

Downloaded From: https://proceedings.asmedigitalcollection.asme.org on 06/28/2019 Terms of Use: http://www.asme.org/about-asme/terms-of-use

Pseudo-Rigid-Body Model

Since Pivot-Arm CVT configurations use compliant members for their internal spring force, a brief explanation of compliant mechanism theory and the pseudo-rigid-body model is presented here. Because the compliant members go through very large deflections, they fall outside the boundary of small deflection approximations that are typically used in rigid body analysis.

The calculations used for large deflection analysis are usually non-linear and can be cumbersome. To overcome the difficulties of large deflection analyses, the Pseudo-Rigid Body Model (PRBM) was developed (Howell 2001). In the PRBM, compliant members are replaced with rigid links connected by pin joints. The lengths of the rigid links are calculated in such a way that the rigid mechanism's end point path is the same as the compliant member's. Springs are used in conjunction with the pin joints to approximate the force-deflection relationship of the replaced compliant member. A common PRBM that will be used in this research is the simple cantilevered beam with a force at the free end, as seen in Figure 7(a), often referred to as a fixed-pinned mechanism. Its rigid body replacement consists of a rigid link fixed to ground, pinned to a second link with a torsion spring at the joint as seen in Figure 7(b). The relationship between the lengths of the rigid links and the length of the original compliant member is represented by the variable γ and is shown in Figure 7(b). The value of the spring constant at the characteristic pivot is:

$$K = \gamma K_\Theta \frac{EI}{l} \tag{1}$$

where γ and K_Θ are constants that depend on the loading condition.

Another common configuration is the parallel motion or the fixed-guided set-up. The segment is fixed at both ends, with the constraint that the ends remain parallel throughout the deflection of the segment (See Figure 8(a)). The analysis of this PRBM can essentially be broken down into two fixed-pinned segments (See Figure 8(b)). The spring constant for this characteristic pivot is:

$$K = \gamma K_\Theta \frac{\frac{EI}{l}}{\frac{1}{2}} = 2\gamma K_\Theta \frac{EI}{l} \tag{2}$$

Evolution of the Pivot-Arm CVT Configuration

The CVT design that initiated this research is also an example of a self-adjusting CVT (See Figure 9). Like the prototype CVTs examined later, this CVT was designed to replace the front sprockets on the crank of a bicycle. The theory behind this design is that when the load to the bicycle increases, it will be transferred as increased tension in the chain to the CVT. This increased tension will cause the arms of the CVT to deflect effectively reducing its radius. Because this CVT responds to changes in the output torque requirements, it falls into the category of a torque sensing CVT.

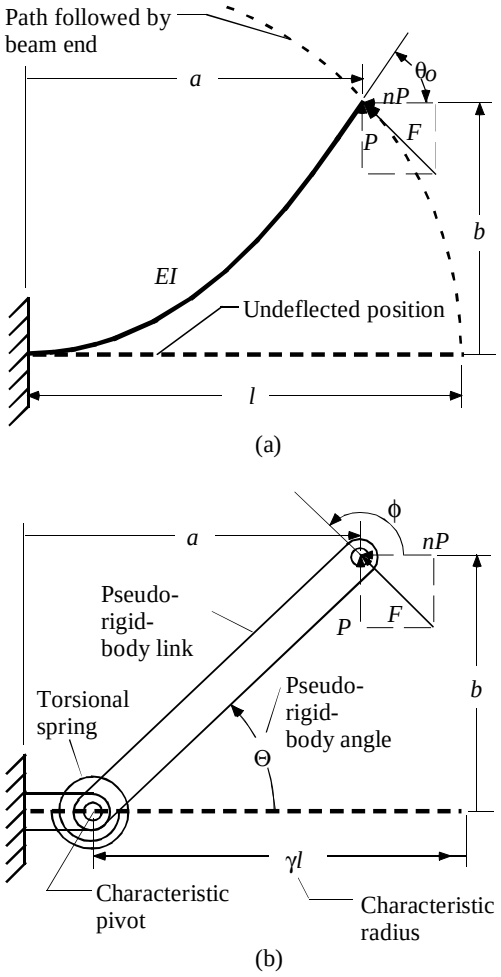

Figure 7: Pseudo-Rigid Body Model for a Fixed-Pinned segment (from Howell 2001)

There are two major shortcomings of this design. First, because the distance between the ends of the arms changes non-incrementally, the chain jumps off the teeth because it needs slack, or falls off because there is too much slack. The second problem is that each arm deflects independently of all the others, causing the energy stored during deflection to be lost when it disengages from the chain.

The research by Mortensen, 2000, that proceeded from this initial CVT design yielded a variety of designs for self-adjusting CVTs. The final prototype of his research is shown in Figure 10. This design works on the same principles as the prototype shown in Figure 9, however it replaces teeth with small sheaves (and uses a belt drive) to overcome the problems with slack. It uses four-bar linkages to solve the problems associated with the lack of dependency between the arms. This prototype led to the development of the category called "Pivot-Arm CVT."

Copyright © 2002 by ASME

Downloaded From: https://proceedings.asmedigitalcollection.asme.org on 06/28/2019 Terms of Use: http://www.asme.org/about-asme/terms-of-use

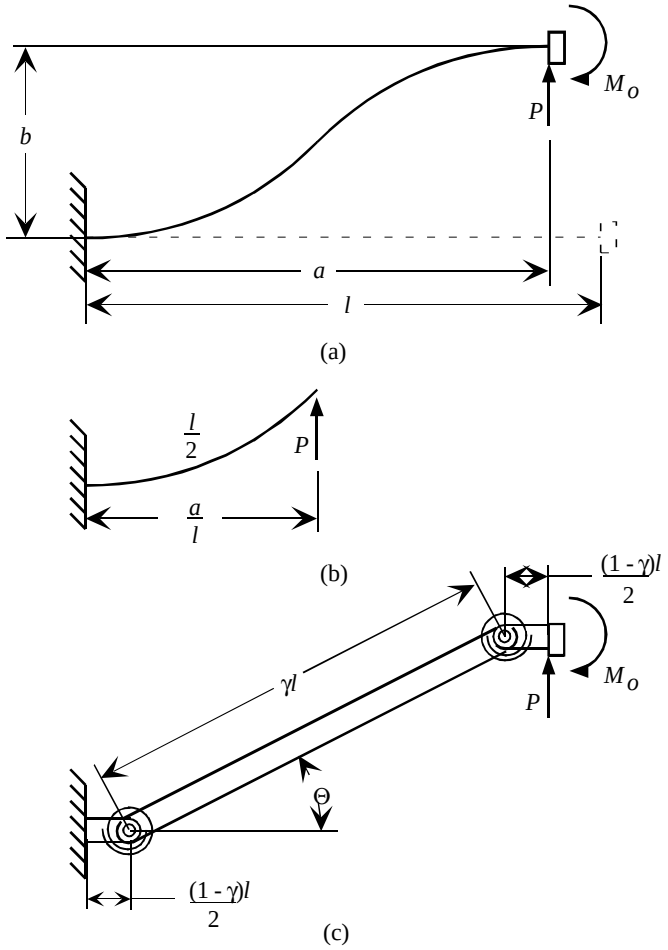

Figure 8: Pseudo-Rigid Body Model for a Fixed-Guided segment (adapted from Howell 2001)

Figure 9: Independent arm CVT design

Figure 10: Parallel Station CVT

Model Development

Through this research a model was developed to predict the performance of the Pivot-Arm CVT configuration. The model will be derived using the basic geometric properties of the generalized Pivot-Arm CVT in conjunction with an approximation of the loading conditions and the internal forces of the CVT. The general model will not address dynamic issues of vibration or harmonic motion. These issues will be explored through testing.

Classification Requirements

The Pivot-Arm CVT consists of a transmission whose driving mechanism has several "stations". Each station is made up of the base and an arm that is attached to the base on a pivot (See Figure 11). The distance from the center of the base to the pivot is denoted by r_g , and the length of the arm attached at the pivot is represented by r_p. The driving mechanism transfers input torque via a chain or belt that rides on the end of each pivot-arm (sprockets would be used with a chain, and sheaves would be used with a belt). The distance from the center of the CVT's input shaft to the end of the pivot-arm is represented by the letter *r*; this value is known as the effective radius.

The general equations that will be developed below can be applied to any Pivot-Arm CVT which satisfy the constraints listed in Table 1.

Copyright © 2002 by ASME

Downloaded From: https://proceedings.asmedigitalcollection.asme.org on 06/28/2019 Terms of Use: http://www.asme.org/about-asme/terms-of-use

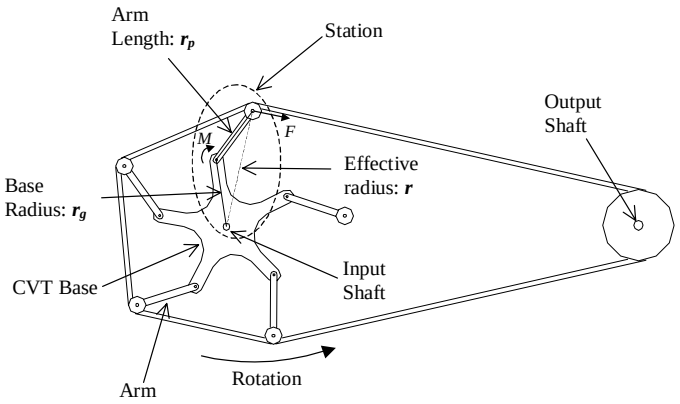

Figure 11: General form of the Pivot-Arm CVT

TABLE 1 Pivot-Arm CVT Criteria

1. The Base Radius, r_g, and the Arm Length, r_p, must both have constant lengths (See Figure 12). A rigid link is the most common example of a constant length, but it can also be achieved by other means.
2. The CVT must have an internal moment, M, that biases the motion of r_p against the applied load, F. This bias can be achieved by means of a spring or other compliant mechanism.
3. Each station of the CVT must be dependent on all of the other stations. In other words, the Load Point of each station must move together with each of the other stations, so that the effective radius, r, is always the same for all of the stations.

Beyond these constraints, the CVT can be configured in whatever manner is most convenient for the mechanisms requirements.

Load Angle Approximation

Figure 12 shows the location of the applied force on the CVT and the CVT's internal moment. The internal moment, M, is shown as a moment about the pivot point. The applied force is shown as F and it is applied at the end of the pivot arm. The applied force is shown in Figure 12 as being perpendicular to the radius vector, r. This is an approximation of what actually occurs during the operation of the CVT. In reality, F is perpendicular to the radius vector with a variation of plus and minus π/n where n is the number of stations on the CVT. Figure 13 shows the transition of each station as it carries the applied load. The station first receives the load as it engages the chain. The station will carry the load until the adjacent station behind it engages the chain. At this point, the first station no longer carries a load.

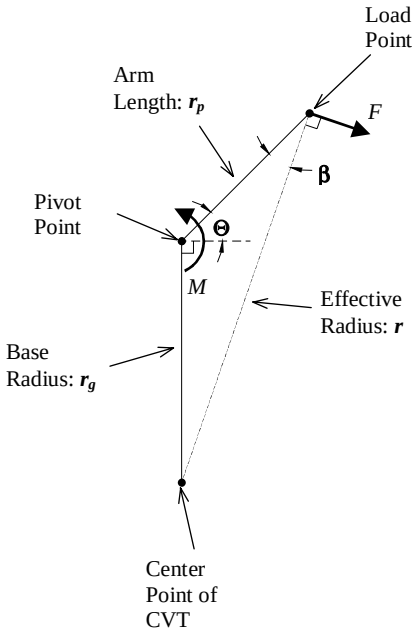

Figure 12: General form of the Pivot-Arm CVT for one station

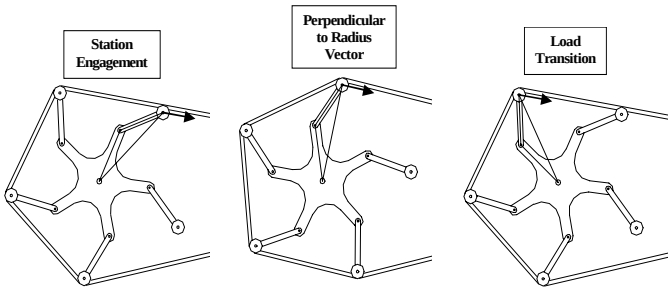

Figure 13: Load transition for a single station

Figure 14 shows the forces from Figure 13 superimposed on the radius vector. This shows that the angle of the applied force varies. Representing the applied force as perpendicular to the radius vector is an approximation to simplify the model.

Equations

From this general CVT model the equations that predict its performance can be developed. Because r_p is rigid, only a portion of the applied load acts against the moment M. The component of the force F that acts against the moment M is F_T,

Copyright © 2002 by ASME

Downloaded From: https://proceedings.asmedigitalcollection.asme.org on 06/28/2019 Terms of Use: http://www.asme.org/about-asme/terms-of-use

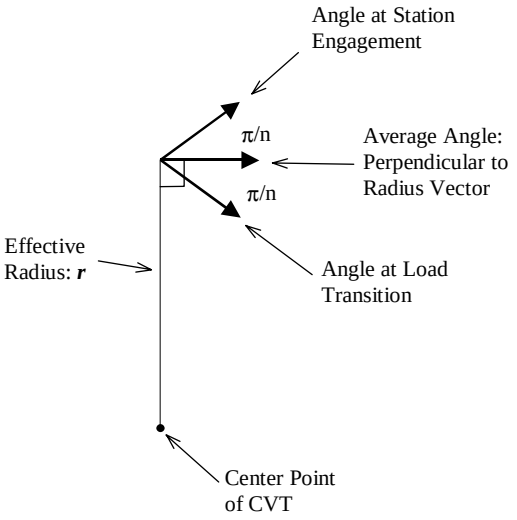

Figure 14: Range of the angle of the applied load

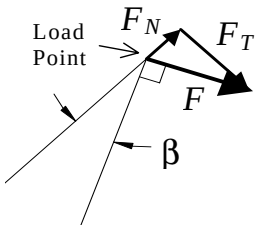

Figure 15: Normal and Tangential components of the applied force

which is the portion that is tangent to the path of the Load Point (See Figure 15).

To maintain equilibrium in the mechanism there must be an equal force caused by the moment, M, that acts opposite to F_T. That force is:

$$\frac{M}{r_p} = F_T \tag{3}$$

The tangent force, F_T, can be expressed in terms of the applied force as follows:

$$F_T = F\sin\left(\frac{\pi}{2} - \beta\right) = F\cos(\beta) \tag{4}$$

The applied force, F, is a function of the applied torque, T, and the moment arm r.

$$F = \frac{T}{r} \tag{5}$$

The goal is to solve these equations to arrive at an expression for the internal moment, M, in terms of the external load, T, and

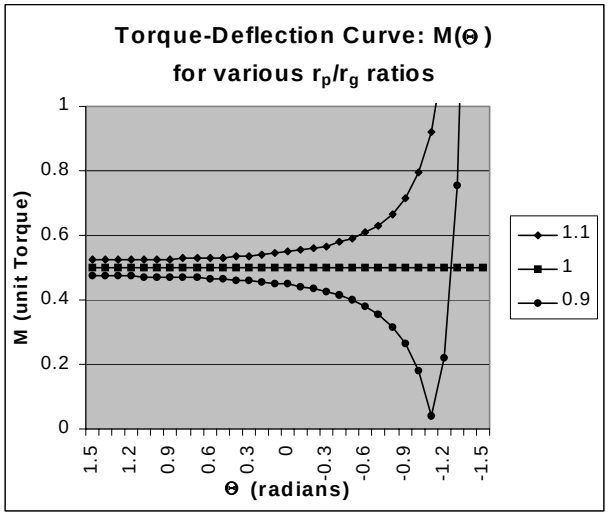

Figure 16: Torque-Deflection curves for various ratios of r_p/r_g

the variable Θ. Substituting Equation (5) into Equation (4) and then inserting that expression for F_T into Equation (3) and solving for M yields:

$$M(\Theta) = \frac{T \cdot r_p}{r} \cdot \cos(\beta) \tag{6}$$

Both r and β are functions of Θ. Using the law of sines, β is:

$$\beta = \operatorname{asin}\left[\frac{r_g}{r} \cdot \sin\left(\frac{\pi}{2} + \Theta\right)\right] \tag{7}$$

Using the law of cosines, r is:

$$r = \sqrt{r_p^2 + r_g^2 - \left(2 \cdot r_p \cdot r_g \cdot \cos\left[\frac{\pi}{2} + \Theta\right]\right)} \tag{8}$$

Substituting Equation (7) and Equation (8) into Equation (6) gives the full formula for $M(\Theta)$:

$$M(\Theta) = \frac{T \cdot r_p}{\sqrt{r_p^2 + r_g^2 - 2 r_p r_g \cos\left(\frac{\pi}{2} + \Theta\right)}} \cdot \cos\left(\operatorname{asin}\left[\frac{r_g}{\sqrt{r_p^2 + r_g^2 - 2 r_p r_g \cos\left(\frac{\pi}{2} + \Theta\right)}} \cdot \sin\left(\frac{\pi}{2} + \Theta\right)\right]\right) \tag{9}$$

Implementation of Internal Moment

The simplest way to create an internal moment as a function of Θ is by using a torsion spring. If it were possible to design a torsion spring with any $M(\Theta)$ curve, then at this point the designer would simply substitute in the values for r_p, r_g, and T, into Equation (9) and then order the corresponding torsion spring. Unfortunately torsion springs have certain torque curve characteristics that will not always match up with the results of this "ideal" torque curve. The next step is to examine the $M(\Theta)$

Copyright © 2002 by ASME

Downloaded From: https://proceedings.asmedigitalcollection.asme.org on 06/28/2019 Terms of Use: http://www.asme.org/about-asme/terms-of-use

1. The output load, T_{out}, is increased.
2. The speed of the input source, S_{in}, begins to decrease because of the increased load.
3. Due to the constant power characteristic of the input source, the input torque, T_{in}, increases.
4. Because T_{in} is above the CVT's operating torque, the transmission ratio, r, decreases. As r decreases, S_{in} increases which causes T_{in} to decrease. The value of r will continue to decrease until T_{in} reaches the CVT's operating torque.
5. At equilibrium T_{in} and S_{in} have both returned to their operating levels, while r has decreased to handle the increase of T_{out}.

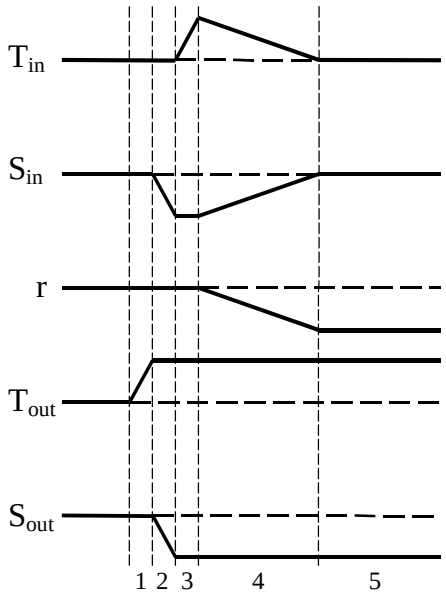

Figure 17: An event sequence for the CVT illustrating relative changes in operating parameters with a change to output torque. The event numbers are described on the left. The event band widths are relative.

curve to determine the possibility of using a traditional spring to create the internal moment, M. An examination of Equation (9) shows that the value for r in both instances is coupled with either r_p or r_g. Therefore, the sensitivity of the function $M(\Theta)$ to changes in r_p and r_g is linear. In other words, the shape of the $M(\Theta)$ curve is the same for any r_p/r_g ratio, only the magnitude of the moment changes with different values for r_p and r_g. Therefore it is helpful to show the curve of $M(\Theta)$ for several values of the ratio r_p / r_g (See Figure 16).

This $M(\Theta)$ curve is the desired curve of a theoretical spring that would be implemented in the CVT mechanism. The closer the actual spring's torque-deflection curve can come to the $M(\Theta)$ curve, the better the functionality of the CVT. If the spring's torque-deflection curve is the same as the $M(\Theta)$ curve, that means that the CVT has a constant torque capacity regardless of the effective diameter at which it is operating.

Constant Torque Rationale

The ideal torque-sensing CVT operates at a constant input torque because this allows the loading source (be it human body or other motor) to adjust the CVT to the ideal effective diameter. This will occur any time the load comes from a source that maintains a constant or near constant power. For a given output speed of the CVT and the torque required to maintain that speed, there is a corresponding power input that is required. Assuming that the CVT is designed to operate at the input source's ideal torque, then the requirement that *power in* must be greater than or equal to *power out* determines the speed of the input source. If the load should suddenly increase, this would cause a decrease in the speed of the input source. For constant power, this decrease in speed would cause an increase in torque which would decrease the effective diameter of the CVT causing an increase in the mechanical advantage of the CVT system. The input source will then reach an equilibrium point at the ideal torque and speed, with the output speed being lower and the output torque being higher than before (See Figure 17).

The opposite occurs if the load is suddenly removed, the source's speed will increase causing a drop in torque. This

Copyright © 2002 by ASME

Downloaded From: https://proceedings.asmedigitalcollection.asme.org on 06/28/2019 Terms of Use: http://www.asme.org/about-asme/terms-of-use

1. The output load, T_{out} , is decreased.
2. The speed of the input source, S_{in} , begins to increase because of the decreased load.
3. Due to the constant power characteristic of the input source, the input torque, T_{in} , decreases.
4. Because T_{in} is below the CVT's operating torque, the transmission ratio, r, increases. As r increases, S_{in} decreases which causes T_{in} to increase. The value of r will continue to increase until T_{in} reaches the CVT's operating torque.
5. At equilibrium T_{in} and S_{in} have both returned to their operating levels, while r has increased because of the decrease of T_{out} .

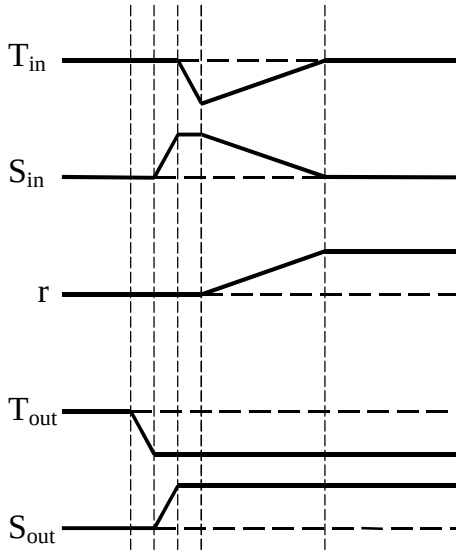

Figure 18: An event sequence for the CVT illustrating relative changes in operating parameters with a change to output torque. The event numbers are described on the left. The event band widths are relative.

decrease in the input torque allows the effective diameter of the CVT to increase, thus decreasing the mechanical advantage of the system. The input source will again reach equilibrium at its ideal torque and speed with the output torque being lower and the speed being higher than before (See Figure 18).

Design Considerations for the Pivot-Arm CVT

This section examines two specific design considerations that will be helpful to the engineer in designing a Pivot-Arm CVT. The first issue that is examined is the situation that exists when the CVT cannot be designed to operate at a constant torque. Next is a discussion of the implementation of a chain and sprockets as the transmission medium. Other design considerations including use of a tensioner, the load-offset approximation and maximum rotation of the pivot arm, are examined in detail by Christensen, 2001.

CVT Implementation in Non-Constant Torque Scenarios

Of course, the ideal $M(\Theta)$ curve can not always be duplicated with a real spring, so the resulting CVT may not have a constant operating torque. If this is the case, it falls to the designer to decide what type of curve is the best choice for the application. It would be useful to solve Equation (4.4) for T and substitute in the function $M(\Theta)$ of the real spring that will be used in the CVT, and then graph T as a function of Θ to see the torque carrying capacity of the CVT at different values of Θ. The designer should choose the range of Θ that most closely matches the requirements of the CVT to be designed. For most situations with constant power input sources, the designer should choose the range of Θ where the value of T remains nearly constant (for reasons that have just been discussed).

If the Torque - Θ curve has a constant, positive slope (as typical springs do), the CVT should be designed with the source's ideal torque and speed occurring at the mechanical advantage that would correspond to the system's typical load. In other words, because the mechanical advantage of the system is a function of T, that equation along with the equation for conservation of power in the system can be used to solve for the value of the spring's moment at the value of T corresponding to the necessary mechanical advantage.

With this discussion, a few variables can now be defined that will help with the modeling of the CVT:

Copyright © 2002 by ASME

Downloaded From: https://proceedings.asmedigitalcollection.asme.org on 06/28/2019 Terms of Use: http://www.asme.org/about-asme/terms-of-use

$T_{out}^{typical}$: Typical output torque required

T_{in}^{ideal} : Ideal torque of input source.

r_{in}^{ideal} : Effective radius of CVT at T_{in}^{ideal}.

r_{out} : Radius of output sprocket.

Θ^{ideal} : Angle of the station at r_{in}^{ideal}.

$M(\Theta^{ideal})$: Moment applied by internal bias at Θ^{ideal}.

The following are two definitions of mechanical advantage:

$$\frac{r_{out}}{r_{in}} = MA = \frac{T_{out}}{T_{in}} \tag{10}$$

Solving Equation (10) for r_{in}^{ideal}, given T_{in}^{ideal}, $T_{out}^{typical}$, and r_{out}:

$$r_{in}^{ideal} = \frac{T_{in}^{ideal}}{T_{out}^{typical}} \cdot r_{out} \tag{11}$$

Subsituting r_{in}^{ideal} for r Equation (8) can be rearranged to solve for Θ^{ideal} giving the expression:

$$\Theta^{ideal} = \operatorname{acos}\left[\frac{r_p^{\,2} + r_g^{\,2} - (r_{in}^{ideal})^2}{2 \cdot r_p \cdot r_g}\right] - \frac{\pi}{2} \tag{12}$$

Using the terms r_{in}^{ideal} and Θ^{ideal} for r and Θ, respectively, in Equation (6) and using Equation (7) along with the terms T_{in}^{ideal} and r_{in}^{ideal} in place of T and r, respectively, yields:

$$M(\Theta^{ideal}) = \frac{T_{in}^{ideal} \cdot r_p}{r_{in}^{ideal}} \cdot \cos\left[\operatorname{asin}\left(\frac{r_g}{r_{in}^{ideal}} \cdot \sin\left[\frac{\pi}{2} + \Theta^{ideal}\right]\right)\right] \tag{13}$$

This is the value of the internal moment at the optimal operating position. This gives enough information to know the specifications of the spring, because the initial assumption was that the spring constant was known.

Chain and Sprocket Implementation

The Pivot-Arm CVT like many other CVTs does not have discrete increments of ratio changes. This means that the distance between the ends of the pivot arms changes continuously rather than incrementally. It would be difficult to use a chain with fixed sprockets at the ends of the pivot arms.

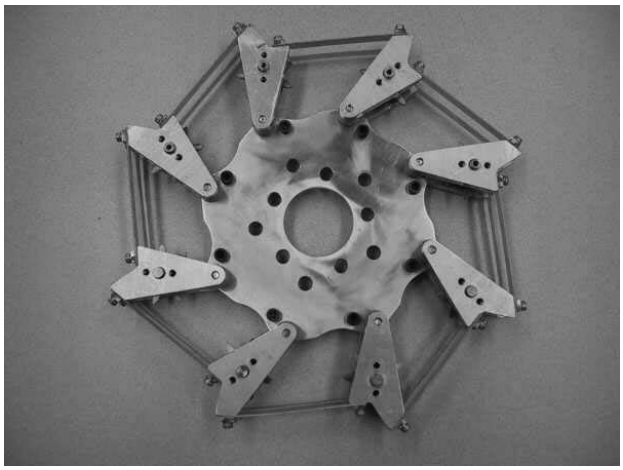

Figure 20: Parallel-Station CVT, adapted with sprockets

Slack would occur in the chain when the radius decreases, and the chain would skip off the sprockets when the radius increases.

The key to the chain and sprocket implementation is the use of a one-way clutch on the axle of each of the sprockets, Christensen 2001. The clutch should be oriented in such a way that it will carry the load when the torque is applied, but will freely allow the chain to move in the opposite direction. This configuration allows the CVT to release excess chain from the system or pull additional chain into the system as needed on a continuous basis.

Testing

Given that the equations that predict the performance of the Pivot-Arm CVT have been developed and explained, they will now be validated through testing. The next step will be to apply these equations to two Pivot-Arm CVT prototypes to determine if they predict actual performance. The prototypes that will be used are the Parallel Station CVT and the Slotted-Plate CVT. If the Pivot-Arm CVT equations accurately describe the performance of these CVT's, then the model can be extended to other CVT applications with reasonable assurance that it is valid.

Parallel Station CVT Prototype

The parallel station CVT is unique because it uses parallel four-bar linkages with a compliant member as the link opposite the ground link to satisfy both the second and third requirements of the Pivot-Arm CVT. The compliance provides the bias against the applied load. The parallel motion and coupling of adjacent four-bar linkages provides the dependency between stations. The parallel station CVT was initially designed with small sheaves fixed to the end of each pivot arm. Because of the losses associated with sheaves and a V-belt, efforts were made to replace the sheaves and belt with sprockets and a chain. The key to making the sprockets and chain (which are discrete in nature) function in a CVT system that is not discrete is the use of roller clutches. The roller clutches allow the sprockets to rotate

Copyright © 2002 by ASME

Downloaded From: https://proceedings.asmedigitalcollection.asme.org on 06/28/2019 Terms of Use: http://www.asme.org/about-asme/terms-of-use

TABLE 2 Parallel-Station CVT Parameters

CVT Geometry		Compliant Strip	
Variable	**Value**	**Variable**	**Value**
r_p	0.051 m	γ	0.85
r_g	0.066 m	K_Θ	2.6
Θ_o	1.05 rad	E	3.90×10^{10} Pa
		I	4.68×10^{-13} m^4
		l	0.060 m

forward to adjust for slack in the chain as the CVT changes in diameter. However, the roller clutches allow the sprockets to carry the applied load because they do not rotate backwards. Figure 20 shows the parallel station CVT prototype adapted with sprockets. The maximum R value for this CVT is 1.24.

CVT Analysis

This CVT configuration can be analyzed Using the set of equations developed earlier. There are several steps in the analysis of a Pivot-Arm CVT. First, the equation for the torque of the CVT as a function of the station deflection, Θ, must be determined. Second, the function for the internal moment must be found and substituted into the expression for the torque. Next, the expression for the CVT's torque is evaluated using the values for the geometry of the CVT and the characteristics of the compliant mechanism. This function of $T(\Theta)$ is then compared to the actual performance of the CVT.

Torque Expression

The internal moment in this CVT is provided by the deflection of compliant strips of E-glass. Therefore, the moment, M, can be determined by using the Pseudo-Rigid Body Model, as will be shown later. Because M is known, the following equation will be rearranged to solve for T as a function of Θ.

$$T(\Theta) = \frac{M \cdot r}{r_p \cdot \cos(\beta)} \tag{14}$$

This expression does not include any of the special design considerations for the adjustment for using a tensioner and the load offset consideration (see Christensen, 2001). To account for these considerations new variables are introduced for M', r', r_p', and β' yielding:

$$T(\Theta) = \frac{M' \cdot r'}{r'_p \cdot \cos(\beta')} \tag{15}$$

For comparison purposes, the predictions for the CVT's torque from both Equation (14) and Equation (15) will be used. Keep in mind that the internal moment, M, is not a constant in these equations, but instead is still a function of Θ, the angular deflection.

Internal Moment

The bias for each station is produced by a compliant strip whose motion is fixed-guided. The definition of a fixed-guided segment is one where both ends of the compliant segment are fixed, and the angle between the beam ends is constant. This type of segment was used for this CVT design because it causes the motion of adjacent stations to be parallel which forces dependency between stations.

The expression for the internal moment of the compliant member can be determined using the principle of virtual work as:

$$M(\Theta) = 4\gamma K_\Theta \frac{EI}{l}(\Theta - \Theta_o) \tag{16}$$

This expression for the internal moment should be substituted into the equation for the torque of the CVT. In the analysis of this prototype there are two equations describing the torque. The first is Equation (14) which does not include the adjustments for the sprockets, and the second is Equation (15) which does include the sprocket adjustments. Both of these equations will be evaluated and compared to test results.

Torque Evaluation

Table 2 shows the two sets of variables that need to be substituted into the equations for the CVT's torque.

Table 3 shows the results of the evaluation of Equation (14) and Equation (15) after substituting in Equation (16) and the values from Table 2. Because each station in a pivot-arm CVT is dependent on all the others, an applied load on a single station is spread equally among all the stations. The Pivot-Arm CVT equations that have been derived in this research only give the

Copyright © 2002 by ASME

Downloaded From: https://proceedings.asmedigitalcollection.asme.org on 06/28/2019 Terms of Use: http://www.asme.org/about-asme/terms-of-use

TABLE 3 Predicted Torque Values

Θ (rads)	Torque (N*m) * From Equation (14) (derivations)*	Torque (N*m) * From Equation (15) (derivations)*
0.6	9.54	5.78
0.5	12.41	7.71
0.4	15.62	9.75
0.3	19.32	11.93
0.2	23.75	14.29
0.1	29.30	16.89

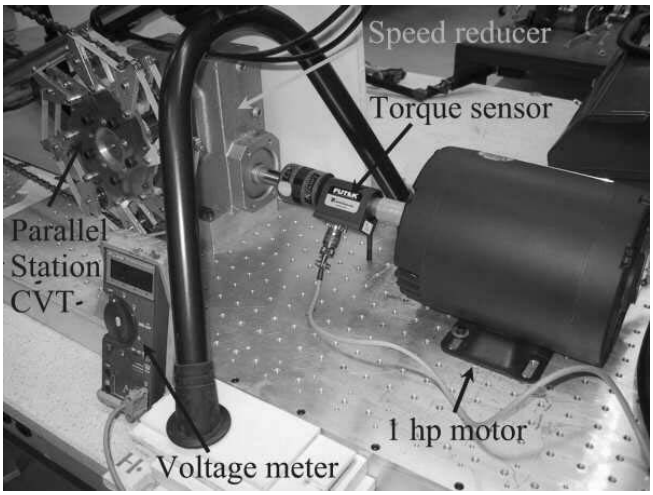

Figure 21: Parallel-Station CVT Test setup

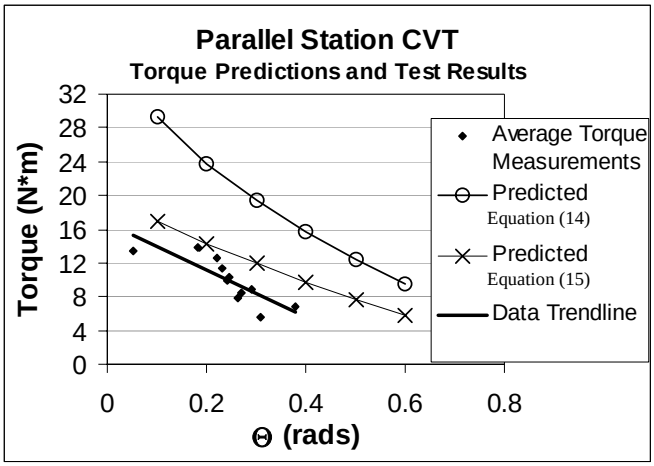

Figure 22: Parallel Station CVT torque predictions and test results

torque for a single station. Therefore, the results listed in Table 3 have been multiplied by eight (the number of stations) to give the torque for the entire CVT. The torque results given in Table 3 are limited to the range of Θ for the parallel-station prototype.

A comparison of the two columns of predictions shows that the predictions using equation 16 are about 30% lower than the predictions without the special considerations for this particular CVT configuration.

CVT Testing

The parallel-station prototype was adapted with sprockets, and torque readings were taken as the CVT was subjected to a load. Figure 21 shows a picture of the test setup. A one horsepower motor was coupled to a 20:1 speed reducer through a torque sensor. The CVT was attached to the output shaft of the speed reducer. A bicycle chain was used to couple the CVT to an exercise bicycle setup. The bicycle was used to have a means of reliably varying the load that was applied to the CVT. The test setup was first run without the load on the CVT to determine the load caused by the speed reducer. Then the load was added to the CVT via the chain, and the test was recorded on video tape. The load was applied via the hand brake to the exercise bicycle. The load was varied in such a way as to achieve the range of the CVT's deflection. Next, the video was captured frame-by-frame on a computer to record the station deflection and torque at several points during the test. Torque measurements were recorded for each quarter turn of the CVT. Because of fluctuations due to the motion of the stationary bicycle, the torque measurements were averaged to reach a single torque value for each full turn of the CVT.

These torque averages are shown graphically in Figure 22 along with the predicted torque curves and a linear fit trendline. The prediction line labelled "Predicted Equation (14)" comes from the data in column 2 of Table 3, and "Predicted Equation (15)" comes from column 3 of Table 3. As can be seen in the graph, the predicted torques are slightly higher than the actual results of the torque test. The trendline shows that the general slope of the predictions is good, and the predictions from Equation (15) are very close to the trendline of the observed data. However, if the model's accuracy can be improved, then the usefulness of this tool to design engineers will be greatly increased.

Copyright © 2002 by ASME

Downloaded From: https://proceedings.asmedigitalcollection.asme.org on 06/28/2019 Terms of Use: http://www.asme.org/about-asme/terms-of-use

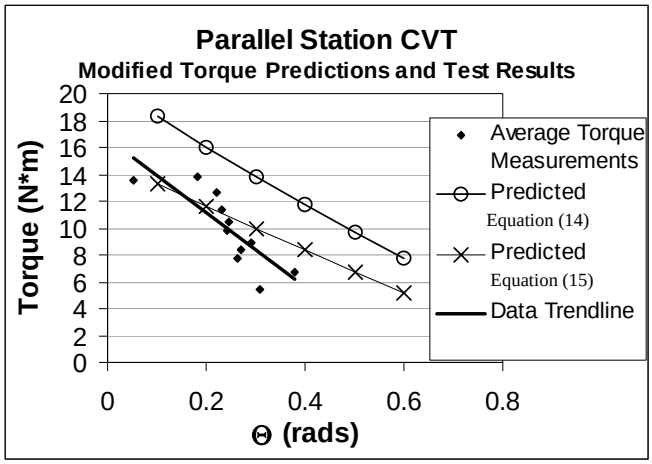

Figure 23: Parallel Station CVT with modified load angle torque predictions and test results

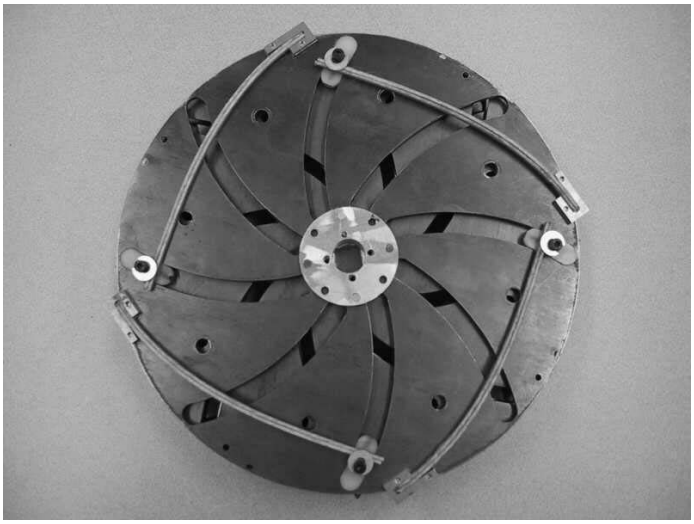

Figure 24: Slotted-Plate CVT Prototype

Modified Torque Predictions

There are other considerations which may have influenced the performance of the CVT. The primary consideration that affects the torque predictions of the CVT is that the load angle approximation is a "middle-of-the-road" approach. The assumption that the load is perpendicular to the radius vector is actually just the average of the conditions that actually exist. A "worst-case" approach may be a more accurate reflection of reality.

To modify the torque predictions, π/n is subtracted from the variable β before it is substituted into the torque equations. The modified torque predictions due to the change in the load angle approximation are shown in Figure 23 along with the data from the torque test. The modified predictions match the observed data quite well. The "Predicted Equation (15)" line is not identical to the data trendline, but is much closer than the previous predictions.

Conclusion

Although the original predictions listed in Table 3 were close to the observed values from the torque test, they did not take into account certain outside influences and behaviors that do not follow the model's assumptions. Modifications to the model due to the load angle approximation yielded predictions that were much closer to the observed data. Because of this, the load angle approximation should be examined further to determine its accuracy in predicting the CVT's behavior.

Slotted-Plate CVT Prototype

Figure 24 shows a picture of the assembled Slotted-Plate CVT prototype. This was the first prototype to explore the idea that the pivot-arm could swing inside the base diameter (in the negative range of Θ). In other words, up until this prototype, the effective radius, r, was always greater than the ground radius, r_g. However, some simple calculations showed that the value of the ratio range, R, is highest as Θ approaches $-\pi/2$. The actual R value for this CVT design is approximately 2.55. Because of this change in the orientation of the pivot arm, the parallel station configuration is not feasible because of interference problems. The internal bias and station dependency must be satisfied another way.

Another interesting point about this CVT design is that it does not use a rigid link to satisfy the first Pivot-Arm criteria of constant length r_p and r_g. Instead, it uses two plates with slots that follow the arc of a pivot arm with constant length r_p. Figure 25 shows a single station on the CVT including the location of r_p, r_g, r, and the effective pivot and load point. So, although there is actually no pivot arm, it still satisfies the Pivot-Arm criteria.

The internal bias was satisfied by several compliant strips per station. The CVT was designed so that the characteristic pivot for the compliant strips coincided with the center-point of the slot's arc. Effectively, this configuration was the same as an actual arm with a torsion spring at its pivot.

The station dependency requirement was satisfied by using a "follower" plate. This plate is similar in appearance to the slotted "base plate" that carries the applied load (See Figure 26 for a comparison). However, the only function of the follower plate is to force the "stations" to always have the same effective diameter. This actually allows the applied load to be equally distributed among all of the stations rather than be carried by a single station only. Figure 27 shows an exploded view of the Slotted-Plate CVT prototype.

An important issue in determining the necessary configuration of the slots on the follower plate is that there should be no

Copyright © 2002 by ASME

Downloaded From: https://proceedings.asmedigitalcollection.asme.org on 06/28/2019 Terms of Use: http://www.asme.org/about-asme/terms-of-use

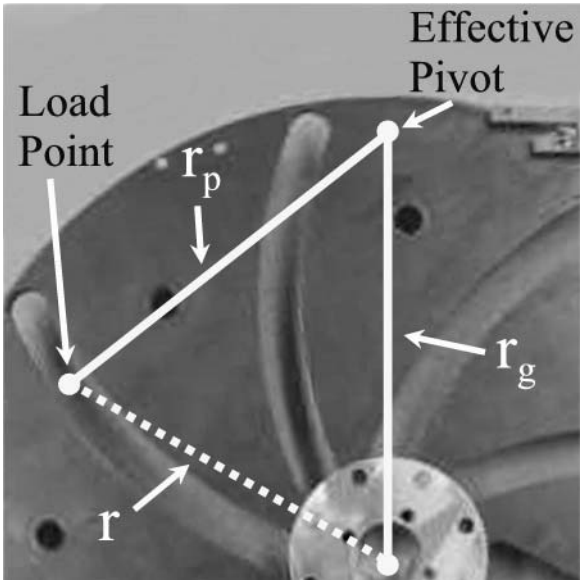

Figure 25: Slotted-Plate CVT station notation

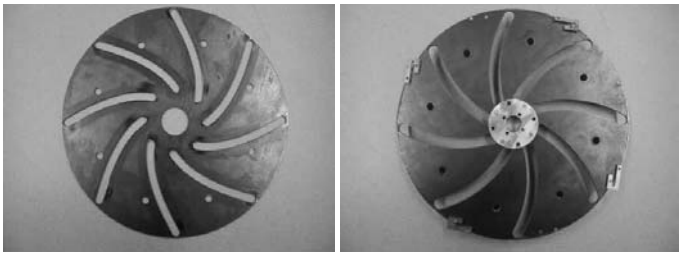

(a) (b)

Figure 26: Slotted-Plate CVT Follower Plate (a) and Base Plate (b)

mechanical advantage in the motion of the plate. There should be a 1:1 ratio between the motion of the station and the motion of the plate at any given moment. This 1:1 ratio will allow for efficient transfer of the force required to cause the dependency of the other stations.

CVT Analysis

Just as with the analysis of the parallel-station prototype there are several steps in the analysis of this prototype CVT. First, the equations for the torque of the CVT as a function of the station deflection, Θ, must be determined. Second, the function for the internal moment must be found and substituted into the expressions for the torque. Next, the expressions for the CVT's torque are evaluated using the values for the geometry of the CVT and the characteristics of the compliant mechanism. These functions of $T(\Theta)$ are then compared to the actual performance of the CVT.

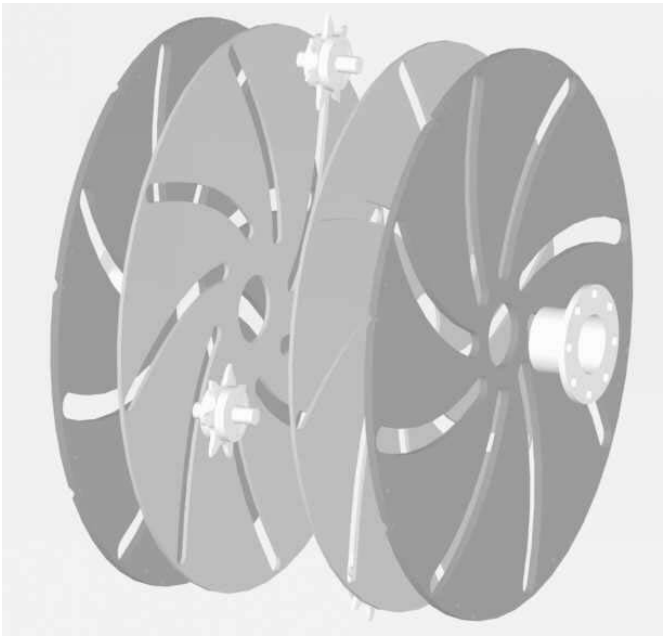

Figure 27: Exploded View of the Slotted-Plate CVT prototype

Torque Expression

The basic expression for the torque of the CVT is the same as Equation (14):

$$T(\Theta) = \frac{M \cdot r}{r_p \cdot \cos(\beta)} \tag{17}$$

As with the parallel-station prototype, this expression for torque does not include same design considerations. The variables M, r, r_p, and β must all be replaced by their alternate values from: M'. The expression for T with the adjustments the same as equation (16) is:

$$T(\Theta) = \frac{M' \cdot r'}{r'_p \cdot \cos(\beta')} \tag{18}$$

Once again, because M is not a constant, the function for the internal moment must be derived and substituted into these equations.

Internal Moment

The Pseudo Rigid-Body Model approximation of a cantilevered beam with a force at the free end is two rigid links connected by a pin joint with a torsion spring at that joint (as seen in Figure 7). The equation for the spring constant, K, is:

$$K = \gamma K_\Theta \frac{EI}{l} \tag{19}$$

The equation for the moment caused by a torsion spring is:

Copyright © 2002 by ASME

Downloaded From: https://proceedings.asmedigitalcollection.asme.org on 06/28/2019 Terms of Use: http://www.asme.org/about-asme/terms-of-use

TABLE 4 Slotted-Plate CVT Prototype Independent Variables

CVT Geometry		Compliant Strip	
Variable	**Value**	**Variable**	**Value**
r_p	0.105 m	γ	0.85
r_g	0.100 m	K_Θ	2.65
Θ_o	0 rad	E	3.90×10^{10} Pa
		I	3.75×10^{-12} m^4
		l	0.124 m

TABLE 5 Predicted Torque Values

Θ (rads)	Torque (N*m) *From Equation (17) (derivations)*	Torque (N*m) *From Equation (18) (derivations)*
-0.7	13.12	10.82
-0.8	14.55	12.21
-0.9	15.67	13.35
-1.0	16.32	14.14
-1.1	16.24	14.43
-1.2	14.99	13.97
-1.3	12.06	12.41

$$M = K(\Theta - \Theta_o) \quad (20)$$

Substituting Equation (19) into Equation (20) gives the expression for the internal moment caused by the compliant strips:

$$M = \frac{\gamma K_\Theta EI}{l}(\Theta - \Theta_o) \quad (21)$$

Now Equation (21) can be substituted into Equation (17) and Equation (18) to yield the expressions for T in terms of the independent variables of the system.

Torque Evaluation

Table 4 shows the two sets of variables that need to be substituted into the equations for the CVT's torque.

Substituting Equation (21) and the values from Table 4 into Equation (17) and Equation (18) gives the results listed in Table 5.

Because all of the equations for the Pivot-Arm CVT that have been developed thus far only give the torque for a single station, the results listed in Table 5 have been multiplied by the number of stations (four in this case) to give the torque for the entire CVT. The values of Θ listed in this table are limited to the range of the slotted-plate prototype.

As can be seen in the table above, for the slotted-plate prototype there is a noticeable difference between the predictions using Equation (16) and Equation (17). However, in contrast to the parallel station prototype, the prediction for the slotted-plate prototype actually intersect as the angle Θ approaches -1.3.

CVT Testing

The slotted-plate prototype was mounted to a test setup to obtain torque readouts as the CVT was subjected to a load. Figure 28 shows a picture of the test setup. A one horsepower motor was coupled to a 20:1 speed reducer through a torque sensor. The CVT was attached to the output shaft of the speed reducer. A bicycle chain was used to couple the CVT to a exercise bicycle setup. The bicycle was used to have a means of reliably varying the load that was applied to the CVT. The test setup was first run without the load on the CVT to determine the load caused by the speed reducer. Then the load was added to the

Copyright © 2002 by ASME

Downloaded From: https://proceedings.asmedigitalcollection.asme.org on 06/28/2019 Terms of Use: http://www.asme.org/about-asme/terms-of-use

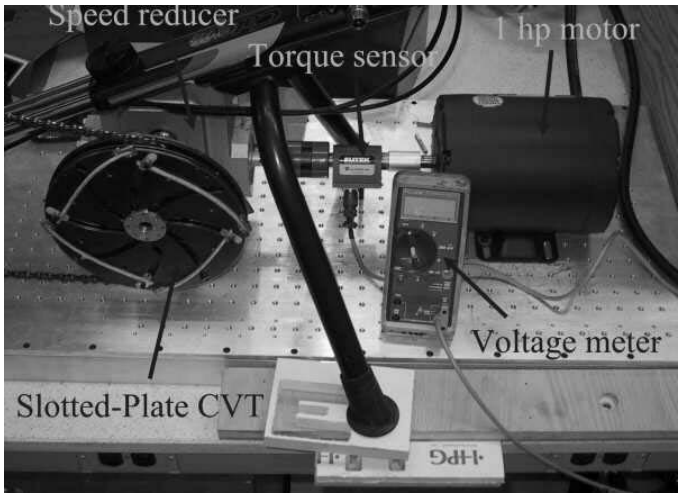

Figure 28: Slotted-Plate CVT Test setup

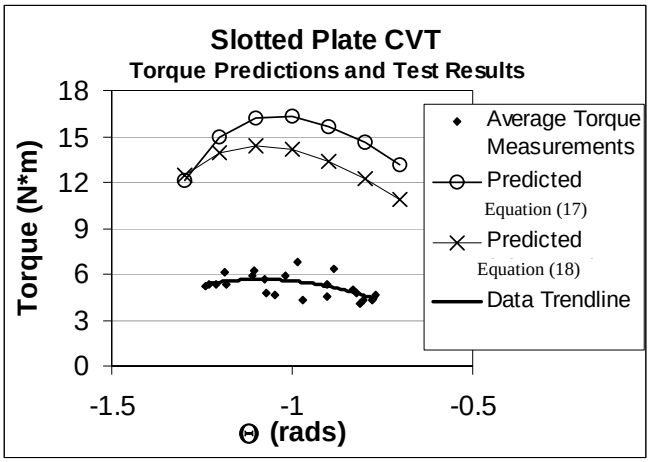

Figure 29: Slotted-Plate CVT torque predictions and test results

CVT via the chain, and the test was recorded on video tape. The load was applied via the hand brake to the exercise bicycle. The load was varied in such a way as to achieve the range of the CVT's deflection. Next, the video was analyzed on a computer to record the station deflection and torque at several points during the test. A torque measurement was recorded every quarter turn. The torque values were averaged in groups of four to reach a torque value for each full turn of the CVT. This was done to remove the fluctuations caused by the movement of the stationary bicycle. The torque averages are shown in Figure 29 along with the prediction curves and a polynomial fit trendline. "Predicted Equation (17)" is the series of predicted values from the second column in Table 5, and "Predicted Equation (18)" is the series of values from the third column of Table 5. It is immediately apparent from these graphs that the predicted torques are considerably higher than the observed torques.

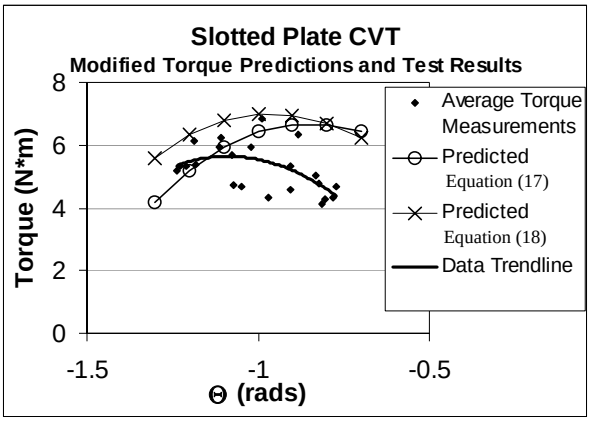

Figure 30: Slotted-Plate CVT modified load angle torque predictions and test results

Modified Torque Predictions

There are other considerations which may have influenced the performance of the CVT. The largest influence is that the load angle approximation is a "middle-of-the-road" approach. As seen in Figure 14, the assumption that the load is perpendicular to the radius vector is actually just the average of the conditions that actually exist. A "worst-case" approach may be a more accurate reflection of reality. To modify the torque predictions, π/n is subtracted from the variable β before it is substituted into the torque equations. The modified torque predictions due to the change in the load angle approximation are shown in Figure 30 along with the data from the torque test. The modifications mentioned bring the predicted torque curves much closer to the trendline from the test data. The results follow the curves for the modified predictions very closely (allowing for effects such as lag time and friction).

Slotted Plate CVT

It is interesting to note that the equations for torque yielded predictions that were much closer to the observed data for the parallel station prototype than for the slotted-plate prototype. The load angle approximation was more accurate for the parallel station configuration because it has eight stations rather than four. Therefore the angle range of the applied load is not as large for the parallel station prototype as for the slotted-plate prototype and does not affect the model's predictions as much. In addition, the compliant strips on the parallel station prototype are much wider and shorter, which gives each station a larger internal moment. This means that, by comparison, the parallel station prototype is much less susceptible than the slotted-plate prototype to effects that are not considered in the model such as friction.

Copyright © 2002 by ASME

Downloaded From: https://proceedings.asmedigitalcollection.asme.org on 06/28/2019 Terms of Use: http://www.asme.org/about-asme/terms-of-use

Conclusions

This research has yielded a model for predicting the performance of the pivot-arm CVT. This model is a useful tool to design engineers. It will aid them in designing pivot-arm CVTs that meet a certain set of performance criteria. The Pivot-Arm CVT model can be used by design engineers in two ways: as a development tool and as a testing tool. First, given the requirements of a transmission system, the model that has been developed through this research can help a designer to develop a pivot-arm CVT that meets those requirements. Second, if a CVT that meets the Pivot-Arm classification criteria has already been developed and built, the Pivot-Arm model can be used to predict the performance of that CVT.

In addition, this research has shown that the Pivot-Arm CVT model is also an accurate prediction model for CVTs that meet the pivot-arm criteria. Testing has shown that with alterations to one of the basic assumptions (load angle approximation assumption), the model is a useful predictor of performance.

The primary advantage of the Pivot-Arm CVT is its ability to automatically adjust the transmission ratio of the system without any user intervention. The CVT adjusts its effective radius based on the level of the input torque. If the input source can maintain constant power through a range of speeds (like a DC motor or the human body), then the CVT is actually adjusting itself in response to changes in the load on the system.

The Pivot-Arm CVT category describes a certain configuration of CVT that is intentionally designed to be self-adjusting based on the input torque. The self-adjusting characteristic is the main advantage of the Pivot-Arm CVT over other types of CVTs. This means that the Pivot-Arm CVT is best suited for applications where other feedback and control methods are impractical. The fact that this CVT is self-adjusting can also be a disadvantage depending on the application. The transmission ratio of this CVT cannot be precisely controlled by the user. And because the feedback and control system is completely mechanical, it is affected by such things as friction and harmonic motion.

The Pivot-Arm configuration has shown potential to be a viable CVT for implementation in a bicycle application. However, this type of CVT could also be used in a variety of other applications. For example, it could be coupled with the motor in a ventilation unit. The motor in this system is chosen for the highest load that it will need to take, which is often the initial start up of the fan. If a smaller motor coupled with a pivot-arm CVT could drive the high initial start up load, then this would represent a large cost savings in manufacturing of the ventilation system.

Acknowledgements

This work was sponsored by Recreation Systems Inc. and the State of Utah Centers of Excellence Program. The authors acknowledge the work of Megan McAllister in the preparing and formating of the paper.

References

Beachley, Norman H. and Frank, Andrew A., *Continuously Variable Transmissions: Theory and Practice*, Lawrence Livermore Laboratory, Livermore, CA, 1979.

Christensen, Myles T., “Analysis of Pivot-Arm Continuously Variable Transmissions,” MS Thesis, Brigham Young University, Provo, UT, 2001.

Hewko, Lubomyr O., “Automotive Traction Drive CVTs - An Overview,” SAE Technical Paper Series, *SAE Passenger Car Meeting and Exposition*, Dearborn, MI, 1986, Paper No. 861355.

Howell, Larry L., *Compliant Mechanisms*, John Wiley and Sons, New York, NY, 2001.

Kluger, Michael A., and Fussner, Douglas R., “An Overview of Current CVT Mechanisms, Forces and Efficiencies,” SAE Technical Paper Series, *1997 Transmission and Driveline Systems Symposium*, Warrendale, PA, 1997, Paper No. 970688.

Mortensen, Clinton R., “Behavior Models For Compliant Continuously Variable Transmissions,” MS Thesis, Brigham Young University, Provo, UT, 2000.

Oliver, L. R., Hornung, K. G., Swenson, J. E., and Shapiro, H. N., “Design Equations for a Speed and Torque Controlled Variable Ratio V-Belt Transmission,” SAE Technical Paper Series, 1973, Paper No. 730003.

Singh, Tejinder, and Nair, Satich S., “A Mathematical Review and Comparison of Continuously Variable Transmissions,” SAE Technical Paper Series, *SAE Worldwide Passenger Car Conference and Exposition*, Dearborn, MI, 1992, Paper No. 922107

Copyright © 2002 by ASME

Downloaded From: https://proceedings.asmedigitalcollection.asme.org on 06/28/2019 Terms of Use: http://www.asme.org/about-asme/terms-of-use